Final Report

Issued: March 23, 2010

Grant Number: DE-FG26-07NT43063

Novel Low Temperature Solid State Fuel Cells

Chonglin Chen (PI and Primary Contact), Patrick Nash (co-PI)

Participate Personals: Jian Liu (Grad), and Gregory Collins (Grad)

Department of Physics and Astronomy, University of Texas at San Antonio

One UTSA Circle, San Antonio, TX 78249-1644

Phone: (210) 458-6427; Fax: (210) 458-4919

E-mail: *cl.chen@utsa.edu*

DOE Project Manager: Patricia Rawls

Phone: (412) 386-5882

E-mail: Patricia.Rawls@netl.doe.gov

Contract Number: 43063

Start Date: December 16, 2006

End Date: December 15, 2009

Disclaimer:

Abstract

We have successfully fabricated (PrBa)$Co_2O_{5+\delta}$ and (LaBa)$Co_2O_{5+\delta}$ epitaxial thin film on various single crystal substrates. Physical and electrochemical properties characterizations were carried out. Highly conductive oxygen-deficient double perovskite $LnBaCo_2O_{5+\delta}$ thin films were grown on single crystal (001) $SrTiO_3$ (STO), (001) MgO, (001) $LaAlO_3$ and (110) $NdGaO_3$ substrate by pulsed laser deposition. Microstructure studies from synchrotron X-ray diffraction and Transmission electron microscopy. High temperature transport properties was carried in different atmosphere (O_2,Air, N_2) up to ~900K. Resistance response of (LaBa)$Co_2O_{5+\delta}$ epitaxial thin film was characterized in oxygen, nitrogen and 4% hydrogen over a wide range of temperature from 400°C up to 800°C. To determine the electrode performance and oxygen exchange kinetics of $PrBaCo_2O_{5+\delta,}$ multi-layered thin film based half cell was deposited on $LaAlO_3$(001) substrate. The temperature dependence of the resistance of this half –cell structure was characterized by electrochemical impedance spectroscopy (EIS) within different temperature and gas environments. Anode supported fuel cells, with GCO:YSZ multilayer thin film as electrolyte and PBCO thin film as electrode, are fabricated on tape casted NiO/YSZ substrate. Full cell performance is characterized up to 800ºC.

Table of Contents

Executive Summary

We have successfully fabricated mixed ionic electronic conductive $(LnBa)Co_2O_{5+\delta}$ (Ln=Pr, La) epitaxial thin film on various single crystal substrates and systematically investigate the relationship of processing-microstructure-property. Various phenomena have been discovered and the critical parameters for their practical applications have been identified.

For the first time**,** a novel symmetric half cell, which is based on epitaxial multilayer thin film, are fabricated by pulsed laser deposition. This design paves the way for studing the electrochemical properties of mixed conductive epitaxial thin film electrodes with advanced ionic electrolyte materials, such as $Gd:CeO_2$ and $Sm:CeO_2$. Moreover, by manipulating the deposition conditions, the physicochemical nature of the oxygen exchange and transfer at the surface and interface of mixed conductors can be revealed. This technology will build a solid foundation of knowledge for the design and fabrication of optimized intermediate temperature micro solid oxide fuel cells.

For electrochemical studies, symmetric half cells were fabricated with $PrBaCo_2O_{5+\delta}$ (PBCO) as a electrode and $Ce_{0.8}Gd_{0.2}O_{1.90-\delta}$ (CGO20 with 8% yttria stabilized zirconia(YSZ) interlayer as electrolyte. The polarization resistance of PBCO thin film electrode is investigated by Electrochemical Impedance Spectroscopy (EIS) with respect to temperature, oxygen partial pressure as well as deposition conditions of the electrolyte. The lowest ASR we obtained at 605°C are 0.1 $\Omega\,cm^2$ in pure oxygen and 0.18 $\Omega\,cm^2$ in air. Two cathode processes, including surface and interface, were observed. By modeling the oxygen surface exchange coefficient, a interface region in the electrode is revealed. It is also observed that the epitaxial PBCO electrodes have very fast surface exchange coefficient (0.006cm/s at 598°C) and extremely low activation energy ~0.28eV. The results indicate that the interface resistance could predominately determine the polarization resistance of the electrode and could be minimized by optimizing the deposition conditions of electrolyte. This research provides valuable information for the development of a thin film based high-performance intermediate temperature micro-solid oxide fuel cell (IT-□ SOFC) with operating temperature as low as 500-700°C.

Highly epitaxial $(LaBa)Co_2O_{5+\delta}$ single crystalline thin films were successfully grown on (001) $LaAlO_3$. The microstructure characterizations from X-ray diffraction and electron microscopy indicate that the films are either A-cation ordered or oxygen vacancy ordered and they are highly *a*-axis oriented with cube-on-cube epitaxy. Transport property measurements indicate that the films have typical semiconductor behavior with a novel phase transition and hysteresis phenomena at 540K. In addition, the chemical dynamic studies reveal that the resistance of the film changes drastically with the change of redox environment. A large the magnitude of resistance changes ($\Box R=10^2 \Leftrightarrow 10^6\ \Omega$) is found within an extremely short response time. These phenomena show that the as-grown $(LaBa)Co_2O_{5+\delta}$ films have extraordinary sensitivity to reducing-oxidizing environment and the exceedingly fast surface exchange rate. These results suggest the epitaxial $(LaBa)Co_2O_{5+\delta}$ thin films can be a promising candidate as ultra-sensitive chemical gas sensor and cathode component for IT-SOFC.

We have demonstrate that the $(LnBa)Co_2O_{5+\delta}$ (Pr, La) epitaxial thin films show superior properties over the bulk materials in many aspects such as thermo-stability, surface oxygen exchange coefficients and activation energy, electrical conductivities in both low and high

temperature range also show significant differences with the bulk. Continuous investigations are required to be conducted on the changes in film quality, interface structures and surface electrochemical properties with material parameters (substrate treatments and compositions) and growth conditions (deposition and annealing temperature, processing pressure, deposition rate, and energy density). In addition, a model of activated surface behavior is needed to be set up by using surface science modeling concepts and equations so that we could determine the optimum configuration for experimental testing and practical applications.

Report Details

Objectives

The Objective of this research is to fabricate and acquire fundamental understanding of the physical properties and chemical stability of advanced nanostructured materials when used in multilayered structures for the development of an intermediate temperature solid oxide fuel cell (IT-SOFC).

Accomplishments

1. ***New Cathode Materials Research: Epitaxial thin film of cathode material $PrBaCo_2O_{5+x}$ (PBCO): microstructure and transport properties***

The family of cobalt oxides, most of which show very high conductivity, displays many interesting physical phenomena, such as anomalous magneto resistance effects and spin glass behavior. Partial substitution of alkaline-earth metals for rare-earth metals in perovskite $LnCoO_3$ cobaltates leads to a number of effects associated primarily with the doping/parent atom size difference and the mechanism associated with the charge compensation of acceptors. These effects include a tendency toward A-site ordering, changes in the oxidation state of the cobalt ions, and the development of significant oxygen nonstoichiometry and oxygen ion conductivity. For example, substitution of barium for half of the rare-earth ions leads to the formation of $LnBaCo_2O_{5+\delta}$, double perovskites in which δ may vary from 0 to 1. It has been found that $PrBaCo_2O_{5+\delta}$ (PBCO) has unusually rapid oxygen transport kinetics at low temperatures (300–500 °C), low electrical resistivity and high ionic conductivity, suggesting its application as a cathode in intermediate temperatures solid oxide fuel cells (IT-SOFC). To study the electrode behavior and avoid the complex microstructure issues, the use of dense thin film with well defined microstructure and geometry is one superior approach. We have synthesized highly epitaxial PBCO thin films on single crystal (001) SrTiO3 (STO) by using pulsed laser deposition (PLD). Our as-grown films show excellent single crystallinity and epitaxial behavior in the microstructure studies. The electrical conductivity relaxation (ECR), and isotope exchange and depth profiling (IEDP) measurements reveal that the PBCO films have higher electronic conductivity in the low-temperature region than traditional electrode materials and much faster surface exchange kinetics.

To study the influence of the interface to the microstructure, we have synthesized highly epitaxial PBCO thin films on single crystal (001) MgO, (001) $LaAlO_3$ and (110) $NdGaO_3$ by using PLD. And the X-ray diffraction was performed for macroscopic studies of crystallinity of the as-grown thin film.

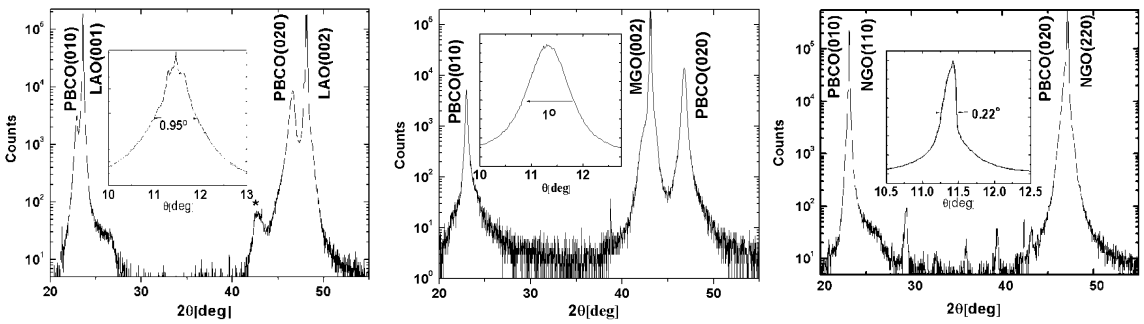

Figure 1 Radial scan of the as-grown PBCO film on (001) MgO, (001) $LaAlO_3$ and (110) $NdGaO_3$ substrate. The inset is a rocking curve measurement from the (010) PBCO reflection.

$PrBaCo_2O_{5+\delta}$ has an oxygen-deficient double perovskite structure, with space group *Pmmm*. Our PBCO target was made with powder prepared by the Pechini method. The pellet was shown to be single phase by powder x-ray diffraction and the cell parameters were determined by Rietveld refinement using the GSAS program to be a=3.9084 Å, b =3.9052Å, and c=7.6343 Å. It can be predicted that PBCO on STO and MGO substrate should grow along the (001) direction. However, due to the development of significant oxygen nonstoichiometry with changes in the

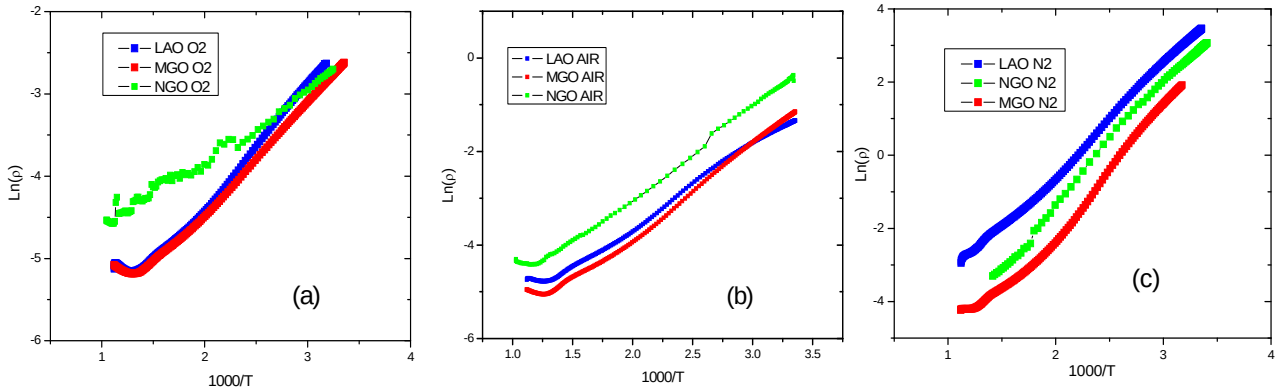

Figure 2 High temperature electrical conductivity for PBCO on various substrates in oxygen, air, nitrogen.

temperature and oxygen partial pressure, the lattice parameters of PBCO will change dramatically with the oxygen content.[38] Under the deposition condition, 800ºC ~850ºC, P_{O2}=250mTorr, the PBCO tends to grow along the *b*-axis on all the substrates even on (001) STO with a, b plane misfit of only -0.05% and -0.005%.The single crystallinity and epitaxial behavior of the PBCO thin films are still dominated by the interfacial crystallography. As shown, the rocking θ scan from the PBCO (010) reflection shows the tilt distribution of the film crystallites with PBCO on NGO having a much narrower tilt distribution than PBCO on MGO and LAO agreeing with the lattice parameters misfit analysis.

Table 1 The lattice misfit between PBCO and single crystal (001) $SrTiO_3$ (STO), (001) MgO, (001) $LaAlO_3$ and (110) $NdGaO_3$ substrate

PBCO	a Å	bÅ	c Å	Δα%	Δβ%	Δγ%
	3.9068	3.9052	7.6343			
STO	3.905	3.905	3.905	-0.05	-0.005	2.3
LAO	3.778	3.778	3.778	-3.29	-3.25	-1.02
NGO	3.859	3.859	3.859	-1.22	-1.18	1.09
MGO	4.213	4.123	4.213	7.83	7.88	10.37

In conclusion, $PrBaCo_2O_{5+\delta}$ thin films have been epitaxially grown on (001) MgO, (001) $LaAlO_3$ and (110) $NdGaO_3$ by pulsed laser ablation. Microstructure studies by X-ray diffraction θ~2θ radial scans and rocking scans reveal that the as-grown PBCO films are b oriented and have excellent single crystallinity. PBCO on (110) NGO substrate has the narrowest tilt distribution of the film crystallites.

High temperature conductivity research

was conducted in tube furnace with custom-made sample holder. The resistance is measured with Lakeshore AC Bridge 370 and a typical four probes method. Experiment was conducted at temperature range of 25-700°C and in 100% oxygen, Air and 100% nitrogen. The resistance measurements on the as-grown PBCO thin films suggest that the electrical conductivities of the PBCO thin films are highly dependent upon the measuring temperature and the interface strain which induce from the lattice mismatch of the films and substrates. The lattice mismatches between the PBCO films and substrates can be simply estimated by the standard crystal lattice parameters.

It is easy to find that the PBCO films are tensile on both NGO and LAO but become strain on MGO. As seen from the Figure 2, the electrical conductivities of PBCO films on these substrates in air have been measured to determine the high temperature transport properties. With the increase of the temperature, the conductivity exponentially increases due to thermal activation and becomes steady around 400ºC (or 670 K) probably owing to the lost of oxygen. It is interesting to note that the PBCO films tensile strain on LAO and NGO substrates have excellent electrical conductivity, ~10^2 S/cm^2, over a very broad temperature region of 300 to 1,000 K. In contrast, the films with relaxed strain on MgO, have relative higher electrical conductivity. In the high temperature range (higher than 400^{o}C), tensile strained films show much better conductivity. Also, compared with the traditional electrode materials such as (La,Sr)MnO_3 or (La,Sr)(Co,Fe)O_3, PBCO thin films have much better electrical conductivity especially in the low temperature region.

2. ***New Electrolyte Materials Research: Gd doped CeO_2:YSZ multilayer thin film electrolyte.***

In comparison with YSZ, pure and doped CeO_2 has significantly higher ionic conductivity and is a candidate for use in SOFCs at lower operating temperatures.[1,2,3,4,5,6,7,8] Whilst an excellent ionic conductor of doped CeO_2, at the fuel side of a cell, ceria based electrolytes suffer from the partial reduction of Ce^{4+} to Ce^{3+} when exposed to low P_{O2} (1×10^{-19} atm) at intermediate temperature (>600 °C). This chemical reaction introduces significant electronic conductivity and results efficiency loss caused by electronic leakage currents between the anode and cathode. It is also accompany with a significant volume fraction which can result in mechanical failure of the electrolyte. The reduction and mixed ionic electronic conduction of ceria has been studied in depth.[9,10] Our approach to address this issue is the integration of ultrathin YSZ blocking layers into $Ce_{0.8}Gd_{0.2}O_{1.90-\delta}$ (CGO20) thin film and achieve to grow YSZ/GCO multi-layer thin film (GCO20/YSZ *ratio = 10:1 and 15:1 and stack number =3 6 and 12*) on (001) MgO by taking advantage of pulsed laser deposition technology. The microstructure, electrical transport properties and the relationship to the design of the hetero-structure were investigated. Fig.3 shows XRD θ~2θ radial scan patterns of GCO/YSZ multilayer films with two different ratios (10:1 and 15:1). All samples showed strong (002) and (004) peaks which suggest a preferred (00l)-oriented phase. And the less intense (111) and (222) peaks indicate the existence of secondary orientations. This feature may due to large lattice mismatch between the film and substrate and the influence of YSZ inter-layers.

A low-magnification, transmission electron microscopy (TEM) image of GCO/YSZ (10:1 x 3) film is shown in Fig. 4. The GCO/YSZ film has a smooth surface, uniform thickness, and a clearly defined interface with the MgO substrate. The columnar-like structure can be clearly observed through the entire film with various domain structures, likely caused by the substrate

surface-step-terrace structure.[11] The interface between GCO and YSZ can not be clearly observed.

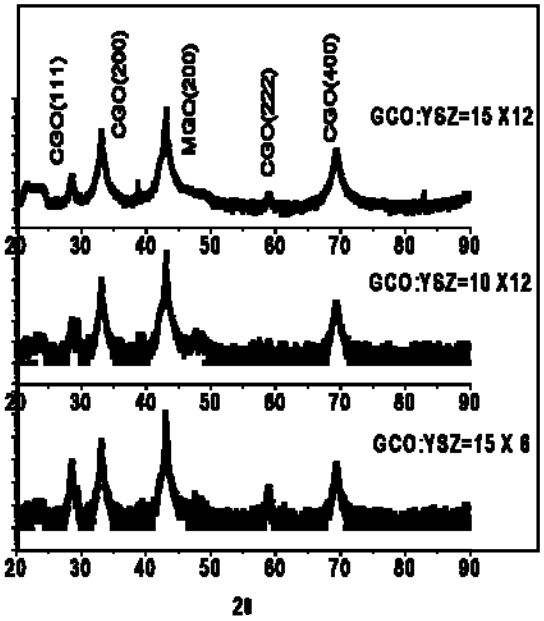

Figure 3 XRD θ~2θ radial scan patterns of GCO/YSZ multilayer films with two different ratios (10:1 and 15:1)

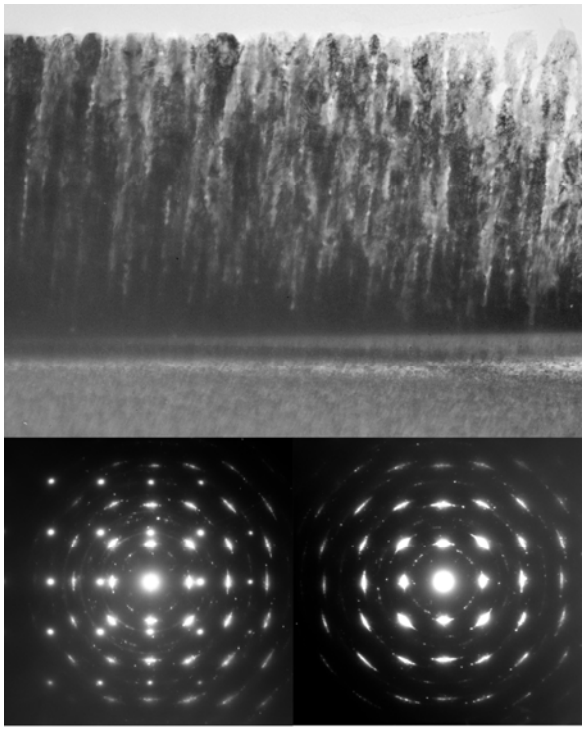

Figure 3 EDP (bottom) and cross section TEM (top) image of GCO/YSZ (10:1 x 3) thin film.

A selected area electron diffraction (SAED) image taken from the area only covering the film and covering both GCO film and MgO substrate along the (001) zone axis of the MgO is shown in Fig. 4. The broadening of the electron diffraction spots from the GCO (200) and (020) reflections and satellite structure show that the GCO film is mostly c-axis-aligned. GCO <111> reflections was not revealed clearly in this pattern.

The resistance and the capacitance were obtained by fitting the data using two parallel RC equivalent circuits. Fig 5 shows normalized typical impedance spectrum on the samples with the same GCO: YSZ ratio (15:1) and different stack number (6 and 12) in oxygen. The spectrum of each sample consist only one arc which is slightly suppressed from the top, indicating the overlap of contributions from grain and grain boundary. The impedance spectrum

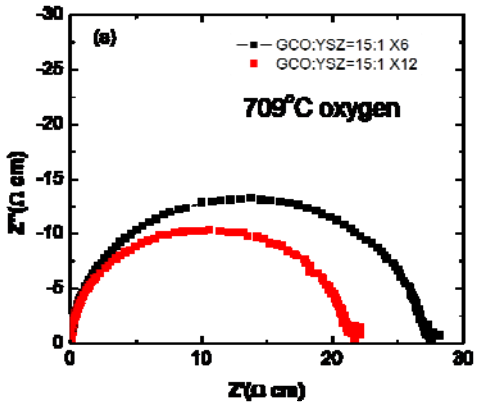

Figure 4 Impedance spectra of GCO/YSZ thin film on MgO

can be fit with an equivalent circuit consisting of two RC components in series. The first component represents the bulk grain contribution, and the second component represents the grain boundary contribution. The impedance spectrum of the YSZ: GCO hetero-structure is expected to contain both due to the layered structure induced phase boundaries. Generally the impedance measurements for grain and grain boundary responses for most oxide materials show capacitance values of ~10^{-12} F or lower and ~10^{-9} F or higher, respectively[12]. From the fitting result of both of the samples, the capacitance corresponding to GCO grain is of the order of 1pF and the capacitance of the grain boundaries is of the order of 1nF. And this result agree very well with the traditional ‘‘brick layer’’ model of grain and grain boundary.

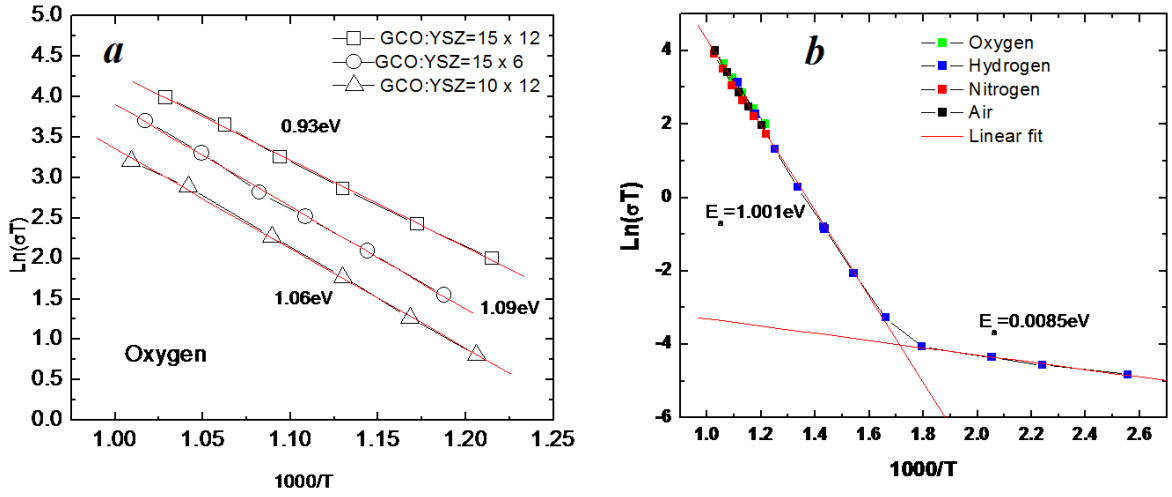

Figure 5 Ionic conductivity of GCO/YSZ multilayer thin film

The ionic transport behavior of Gd doped Ceria and YSZ is usually represented by the equation:

$$\sigma T = \sigma_o \exp(-\Delta E/kT)$$

The activation energy ΔE would have the form $(\Delta H_m + \Delta H_a)$, where ΔH_m and ΔH_a, represent the enthalpy of motion and association enthalpy of the oxygen vacancies and dopant cations defect complex such as $(Gd'_{Ce} - V_O^{\bullet\bullet})$, respectively. At sufficiently high temperatures the defect complexes can be dissociated so that the activation energy of migration of free vacancies would simply be given by ΔH_m. And at intermediate temperatures, ln(σT)-1/T plots should be curved as $[V_O^{\bullet\bullet}]$ is no longer independent of temperature. [13] As shown in Fig 6 (a), the ln(σT) versus 1000/T relationship is linear over the entire temperature range in oxygen, in which the major charge carrier is believed to be $[V_O^{\bullet\bullet}]$. It indicates that the oxygen vacancies and dopant cations defect complexes are essentially dissociated, and also promises the usage as the electrolyte of IT-SOFC. Fig 6(b) shows the result of the samples with GCO: YSZ = 15:1 × 12 tested in oxygen, air, nitrogen, and 4% hydrogen. The conductivity in high temperature range (500°C-800°C) has nearly no change (0.015 ± 0.002 S cm^{-1}, 600°C) in different environments. The activation energy of total conductivity is $0.98 \pm 0.04eV$. Considering the experimental uncertainty, it is can be concluded that the conductivity of the selected sample is independent of

the oxygen partial pressure and the n-type electronic conductivity is reduced significantly by the YSZ inter-layer. This conclusion can also be supported by the measurement in 4% hydrogen (water saturated) in the temperature range of 100°C~800°C as shown in Fig 6(b). It clearly shows two conductive domains which changes around 300°C. In the low temperature range, the conductivity is believed to be dominated by electron migration. The activation energy of low temperature range (100°C-300°C), E_a=0.085eV, which is much lower than that of the ionic conductive domain (1.001eV), can be attributed to the activation energy for electron hopping. The electronic conductivity at 600°C calculated from the fitting result is 3.71×10^{-05} S cm^{-1}, which is about 0.23% of the total conductivity. This result demonstrates that the integration of ultrathin YSZ interlayer in the GCO thin film can significantly enhance the stability of GCO against reducing environment and reduce the electronic conductivity.

3. ***Electrode properties of $PrBaCo_2O_{5+\delta}$ with multilayer thin film based $PrBaCo_2O_{5+\delta}$ /GCO:YSZ/ $PrBaCo_2O_{5+\delta}$ symmetric half cell***

An original symmetric half cell with electrode/electrolyte epitaxy is fabricated by pulsed laser deposition on (001) $LaAlO_3$. $PrBaCo_2O_{5+\delta}$ (PBCO) was selected as a prospective cathode material and $Ce_{0.8}Gd_{0.2}O_{1.90-\delta}$ (CGO) : $Zr_{0.92}Y_{0.08}O_2$(YSZ) multilayer herterostructure was selected as electrolyte. In order to reveal the interface effect, electrodes were deposited with indentical conditions vasus the electrolyte was depositied with two different oxygen partial pressures, 250 mtorr **(Cell 250)** and 300 mtorr **(Cell 300).** Surface-morphology, microstructure, crystallinity, and epitaxial behavior of the as-grown films were characterized by atomic force microscopy, X-ray diffraction (XRD) and transmission electron microscopy (TEM). The polarization resistance of PBCO thin film electrode is investigated by Electrochemical Impedance Spectroscopy (EIS) with respect to temperature deposition conditions of the electrolyte. Both surface and interface cathode processes were observed. The results indicate that in μ–SOFC, the interface process could affect the surface oxygen exchange properties and predominately determines the cathode performance.

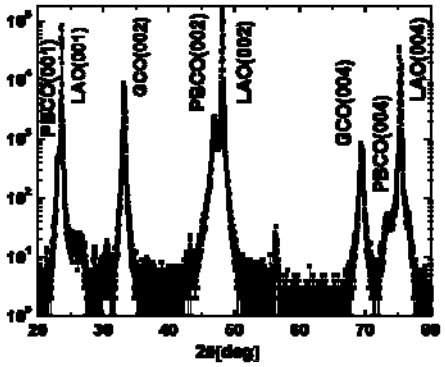

Figure 6 XRD pattern of the as grown PBCO/GCO:YSZ/PBCO film

X-ray diffraction results from the multilayer thin film are presented in Figure 7. Only (00*l*) peaks for GCO, PBCO and substrate appear in diffraction pattern of θ~2θ scan, suggesting that the films are basically c-axis oriented. No peaks for YSZ were observed. To understand the crystallinity and epitaxial behavior, cross-sectional TEM studies have been employed to further investigate the epitaxial quality of the film. Low magnification bright field TEM image (Figure 8 (a)) shows that the as-grown film has sharp interface and good single crystallinity. The half cell structure can be clearly indentified with PBCO as top (200nm) and bottom (125nm) electrodes and GCO:YSZ multilayered electrolyte(350nm). The YSZ interlayer is about 5 nm in thickness.((Figure 8 (c))) The columnar-like growth is a result of the various domains formed at different surface terraces on the substrates. Selected area electron diffraction (SAED) was taken at the interface of PBCO and GCO along a [100] direction of PBCO to study the film quality and

epitaxial behavior. (Figure 8 (b)) The interface relationship has been found to be $(001)_{GCO}$// $(001)_{PBCO/LAO}$ and $<110>_{GCO}$//$<010>_{PBCO/LAO}$, which agrees with the x-ray diffraction studies. The result from HR-TEM also confirms this conclusion. (Figure 8 (d)) It can be concluded that even if the large mismatch in lattice parameter, a_{CGO}=5.40 A and a_{PBCO}= 3.85A (XRD), does not allow a cube-on-cube growth, the epitaxial growth of fluorite oxides on perovskite oxides can be achieved with an in plane rotation of 45 degrees in the (00*l*) axis due to the small mismatch of 0.8% between $d_{220}^{(GCO)}$ and $d_{010}^{(PBCO)}$.(Figure 8 (e)). The broadened diffraction spots of GCO indicate there is minor distored crystal orientation due to the fluorite YSZ interlayers with a_{YSZ}=5.16A. The mean roughness and the surface area difference (measured by atomic force microscope) of as grown top PBCO electrode were 10.3 nm/ 1.62% respectively, which shows a fairly smooth surface.

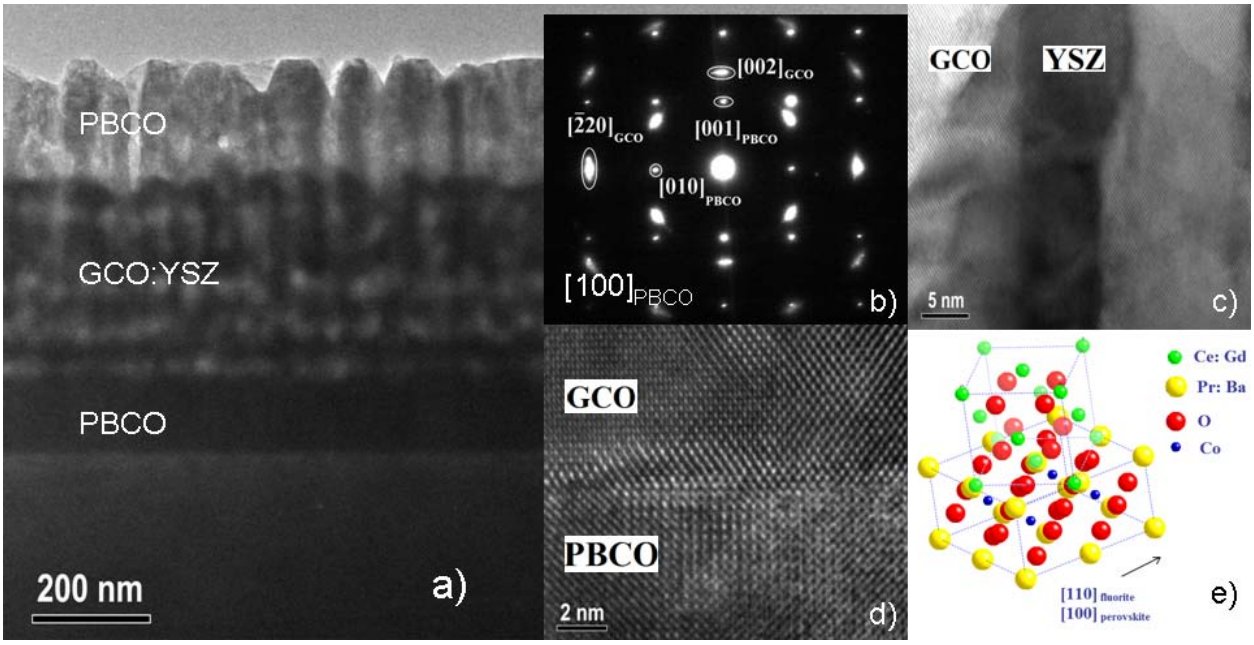

Figure 7(a) Low magnification bright field cross section TEM image of the PBCO/GCO:YSZ/PBCO film; (b) Selected area electron diffraction (SAED) was taken at the interface of PBCO and GCO along a [100] direction of PBCO; (c) HR-TEM image of YSZ interlayer and the YSZ:GCO interface; (d) HR-TEM image of GCO/PBCO interface; (e) Schematic drawing of the epitaxial growth of fluorite oxides on perovskite oxides

Electrochemical impedance spectra were measured on the as grown half cells with two identical PBCO electrodes on top (Figure 9 (a) inset) for temperature rang of 400°C to 600°C. PBCO is an excellent electronic conductor (>400S/cm) and the electric potential is expected to be uniform. The spectra always show an inductive contribution to high frequency and low frequency (LF) arc which represents the polarization resistance of the electrode. A group of selected impedance spectra and modeling results are shown in Figure 9 (a.b). It is believed that for dense thin film MIEC electrodes, the oxygen reduction occurs largely over the electrode surface area, rather than being limited by the triple phase boundary. Therefore, to evaluate the electrode performance, the resistance was only normalized by the surface area. The area specific resistance (ARS) of the cell is calculated from overall electrode resistance by $ARS = R_e \times a \times 1/2$ and plotted as a function of reciprocal temperature in Figure 10 (a), where R_e is calculated by the sum of surface R_s and interface R_i resistance from the impedance spectra fitting results.

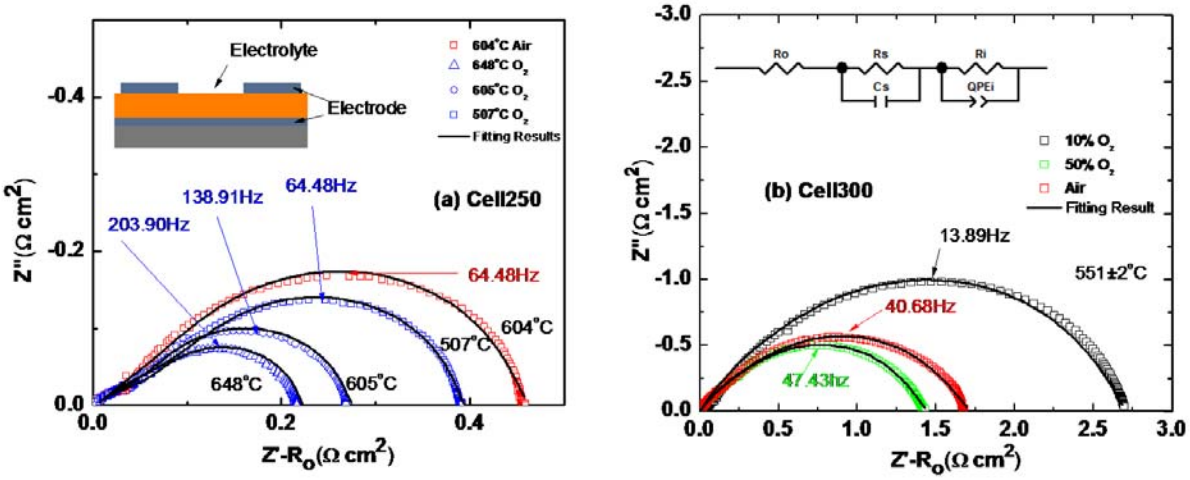

Figure 9 Selected impedance spectra of Cell250 (a) Cell 300 (b); (a) inset: Schematic drawing of the half cell structure; (b) inset: equivalent circuit for the fitting of the spectra.

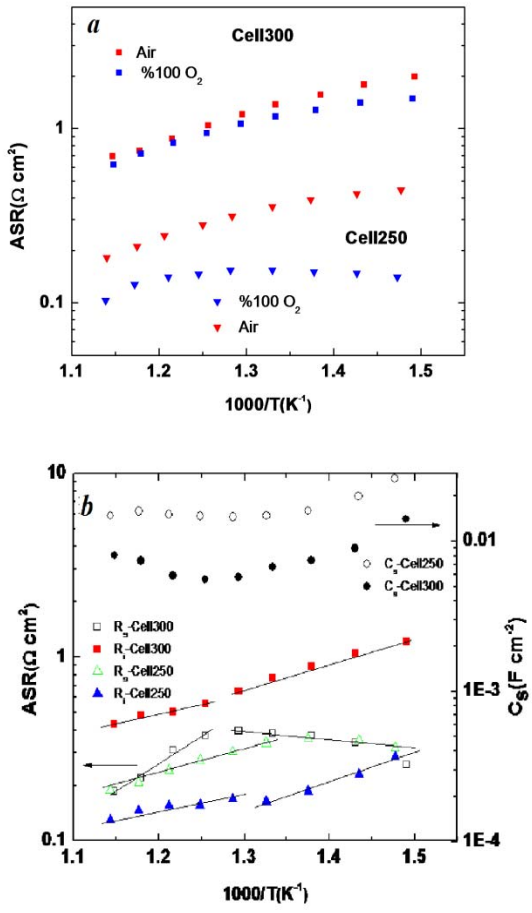

Figure 8 a)The area specific resistance (ARS) in pure oxygen and air; b) fitting results of the interface and surface resistance

The ARS change with temperature clearly shows two regions which agree with the data the bulk sample of PBCO, both ceramic and thin-film, due to the lost of oxygen ion. [9 35]. The lowest ARS we obtained is from Cell250 at 605°C, 0.1 Ω cm^2 in pure oxygen and 0.18 Ω cm^2 in air which is much lower than the recently reported results (0.4Ωcm^2, 600 $^{\circ}$C in air)of polycrystalline $PrBaCo_2O_{5+\delta}$ cathode on samarium-doped ceria electrolyte[21]

The temperature dependence of surface and interface resistance as well as surface capacitance is plotted in Figure 10 (b). The surface resistance R_s of both Cell250 and Cell300 agrees with each other fairly well and implies a very similar surface structure and electrochemical properties. In this Arrhenius plot for R_s, there are two regions which probably represent different reaction mechanisms. with temperature decreasing R_s increases and reach a maximum at 500°C (cell 300) /450°C(cell 250), and then start to decrease. About oxygen exchange and other related reactions on the surface of mixed conducting oxides, conventional wisdom usually assumes that the oxygen dissociation due to an activation barrier is limiting. This seems to fit in our high temperature R_s results with thermo activated behavior. But to explain the phenomena shown at lower temperature range, a different mechanism

must be proposed. One possible reason is that the equilibrium oxygen content of $PrBaCo_2O_{5+\delta}$ is a function of temperature. In pure oxygen, bulk $PrBaCo_2O_{5+\delta}$ has the least oxygen non stoichiometry at about 240°C and start to increases with higher temperature.[20] Similar result has been found for high quality PBCO epitaxial thin films in our research, but the temperature with the max oxygen content varies widely with different substrates and deposition conditions.

Previous studies of dense MICE thin film electrodes on YSZ electrolyte have revealed an intermediate frequencies feature in the impedance spectra.[14] This part of impedance response is attributed to the ionic transfer resistance at the electrode/electrolyte interface. Usually a GCO thin interlayer is inserted between the electrode and electrolyte to see if this is a valid interpretation. However, due to the distinct nature of single crystal YSZ and GCO thin film, the exact nature of this interfacial effect may still be regarded as an open question.

In this project, we took a different approach to address this issue. The thin film based electrolyte layer was deposited under slightly different oxygen partial pressure, so that interface is changed without major influence on the bulk or surface of the electrode. Comparison of impedance data obtained for the Cell250 and Cell300 shows that the intermediate frequencies impedance feature is substantially affected by manipulating the deposition oxygen partial pressure. Compared to R_s, the electrode/electrolyte interface resistance R_i shows a very large difference over the whole temperature range. R_i of cell300 (0.43 Ωcm^2-598C)is much higher than Cell250(0.13 Ωcm^2 -602C) and even higher than the surface resistance of cell300. This phenomenon demonstrates an interface determined electrode resistance in Cell300.

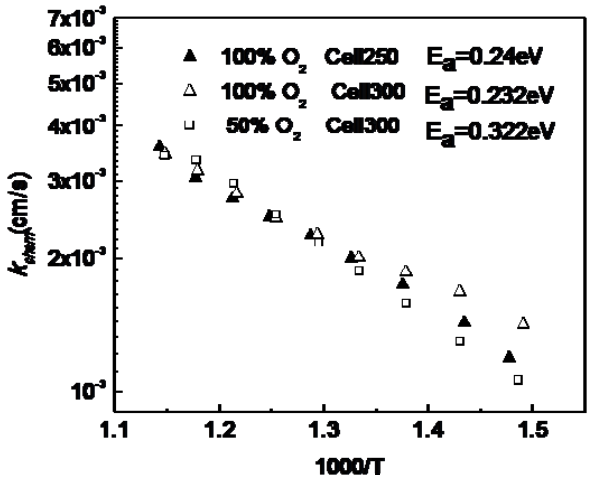

Figure 10 oxygen exchange coefficient and the actvation energy of the PBCO electrode.

To obtain oxygen transport information from the impedance spectra, the first order surface exchange kinetics for the dense thin film can be expressed as [15,16]

$$\omega RC = \omega\tau = 1 \qquad (1)$$

$$k_{chem} = \frac{l}{\tau} = \frac{l}{RC} \qquad (2)$$

Where k_{chem} is the chemical surface exchange coefficient, l is the electrode thickness, τ is the time constant and $\omega = 2\pi f$ is the circular frequency. The activation energy E_a of surface oxygen exchange reaction is calculated from the linear fitting results of k_{chem} between 450~575°C. The lowest E_a, measured from Cell300 in 100% oxygen, is 0.232 eV. This values is only about 1/3 of the bulk PBCO electrode, 0.67eV,[17] and is by far the lowest activation energy ever been reported. This catalytic effect stands in contrast to conventional wisdom, which generally views

O_2 as a difficult-to-activate molecule. It is believed that the exchange rate has a strong Arrhenius dependence cannot be taken as evidence for an activation barrier in the oxygen exchange processes, and the barriers can be partially or wholly entropic (limited by availability of intermediates or sites) rather than energetic.[18] Recent study on the adsorption of atomic and molecular oxygen on the single crystal $LaMnO_3(001)$ surface have revealed that the oxygen vacancy formation and migration enthalpies are much lower than in bulk, so that the concentration and activity of the oxygen vacancies are much higher on single crystal surface.[19] Considering the epitaxial nature of the PBCO thin film, the low activation energy must be origin from the concentrated and activated oxygen vacancies on the single crystal surface. This phenomenon also implies that the barriers to oxygen exchange processes on PBCO may be entropic.

In summary, Epitaxial PBCO/GCO:YSZ/PBCO multilayer thin film based symmetric half cell were fabricated on $(001)LaAiO_3$ substrate by Pulsed Laser Deposition (PLD) method. Electrochemical Impedance Spectroscopy of epitaxial PBCO thin film is measured and analyzed systematically using equivalent circuits. The lowest ARS we obtained at 605°C are 0.1 Ω cm^2 in pure oxygen and 0.18 Ω cm^2 in air. Two cathode processes, including surface and interface, were observed. By modeling the oxygen surface exchange coeffecient, a interface region in the electrode thickness is revealed. It is also observed that the epitaxial PBCO thin film electrodes have very fast surface exchange coefficient (0.006cm/s at 598°C) and extremely low activation energy (0.28±0.04eV). This work demonstrates that in epitaxial thin film based intermediate temperature micro solid oxide fuel cells, electrode/electrolyte interface plays an important role and the interfacial process could affect the surface exchange processes and predominately determines the cathode performance.

4. Development of Full cell and Device Performance

We have constructed anode supported whole cells and conducted characterization and modification of electrolyte layer/ratio composition in order to maximize the ionic transport in the intermediate temperature range. The anode material used is a 50/50 cermet mixture of NiO and YSZ. The nickel has known catalytic properties that are inapplicable to our measurements in a test gas of a 96/4 mixture of N_2 and H_2, respectively. We have obtained a current maximum of approximately 95 mA/cm^2 with an average of 65 mA/cm^2. Calculations of the theoretical cell voltage using the Nernst equation give a voltage of approximately 1.15 volts. Our maximum voltage of approximately 0.91V and average of 0.58V is indicative not only of current leakage but irregularity in our cell production. The problem has been attributed to the inherent porosity and surface roughness of the chosen anode material, allowing presently uncorrectable inter-layer current leakage in random areas of the thin film thereby compromising the insulating property of the YSZ layers. The much lower average than peak voltage is demonstrative of cell inconsistencies that have introduced too much uncertainty in the cell measurements to allow for a thorough investigation of the electrolytical properties.

It can be seen in Fig. 1 that we have been able to produce a current of up to 95 mA/cm^2 with an average of 65 mA/cm^2 at only 4% H_2 + 96% N_2. The measured cell voltage is not as large as that predicted by the Nernst equation:

$$E = E_0 - \frac{kT}{zF}\ln\left(\frac{p(H_2)p(O_2)^{1/2}}{p(H_2O)}\right)$$

where E_0 is the standard cell potential.

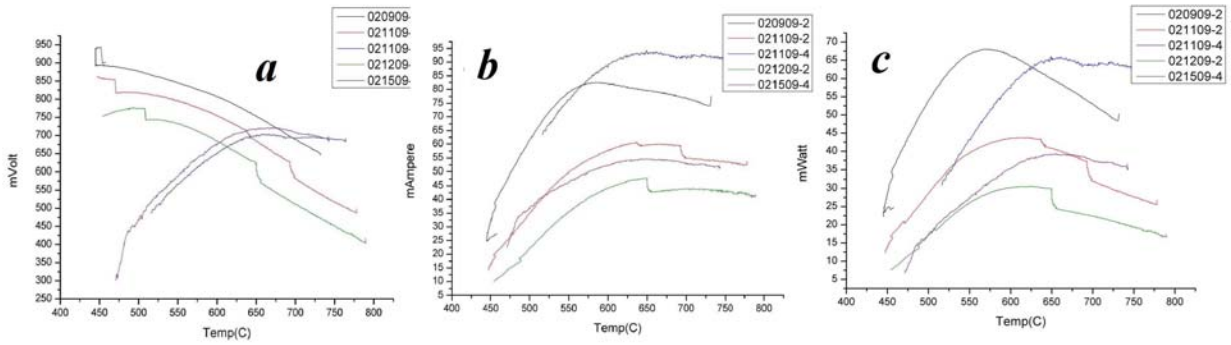

Figure 11 PBCO//GCO:YSZ//NiO:YSZ full cell (a) voltage; (b) current; (c) total power

Calculations of E_0, at the standard equilibrium conditions show that the voltage should be approximately 1.2 volts. With our maximum voltage of approximately 0.9 V (and the majority being considerably less), from Fig. 2, the difference in these voltages must be due to current leakage in the cell. This problem is partially due to the inherent porosity of the anode material and that it has a large amount of surface roughness due to fabrication techniques. We are currently refining our production process to minimize these effects. Another reason for the leakage is due to our uncertainty of the correct thickness for our insulating layer of YSZ as this substrate material poses different deposition challenges than that of our half cells. With these shortcomings, positive results are still seen. While the current peaks between 625 °C and 650 °C, the voltage reaches a maximum at a lower temperature of around 500 °C, resulting in a peak power being realized between 575-625 °C. This is our expected temperature for this electrolyte combination. We plan to test the cells under different fuel gas combinations to see the dependency of the power curve on hydrocarbon molecular size.

Several attempts have been made to condition the anode surface to allow for electrolyte intra-layer integrity. Polishing to a 0.1 finish, however the difference in hardness of the NiO and Y:ZrO_2 caused a micro-sized rippling on the substrate thereby counteracting any benefits obtained form the polishing process and still left micron sized pores. The next attempt was an application of nanoparticles (30-50nm) of YSZ onto the polished substrate surface. This method also had shortcomings, possibly due to the creation of an insulating ZrO_2 layer at the substrate surface or the creation of a high potential barrier due to poor bonding of the YSZ with the substrate. It is believed that there may be a chemical treatment that may provide a suitable surface, however this is still under investigation. We alternatively adopted amorphous metallic ribbon types with double phases as the new anode materials for the cell development. However, due to the time and UTSA travel limits, we cannot complete fuel cell project at this moment but will continually approach it in the near future. Results will be reported soon.

5. ***Search new materials for low temperature solid state fuel cells***

We has achieved the highly epitaxial 112-type layered perovskite $LaBaCo_2O_{5+\delta}$ single crystalline thin film on (001) $LaAlO_3$ by using pulsed laser deposition (PLD). we studied the epitaxial nature and transport properties as well as the kinetic phenomena observed from the as-grown $LaBaCo_2O_{5.5+\delta}$ film. Various interesting phenomena have been found in the films such as extraordinary sensitivity to reducing-oxidizing environment, exceedingly fast surface exchange rate, etc which results in the epitaxial LBCO thin film as a promised candidate for ultra-sensitive chemical gas sensor and/or cathode component in IT-SOFC.

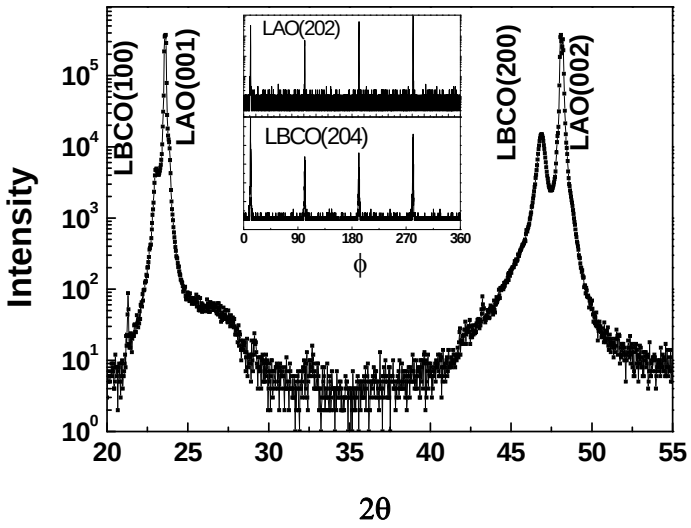

Figure 12 XRD pattern of as grown LBCO film. Inset: Φ scan of LAO substrate and LBCO films

Figure 13 shows the XRD θ–2θ scans of the as-grown LBCO thin film deposited on LAO (001). The as-grown film is pure LBCO phase with highly oriented along the *a* axis with only (*l*00) peaks. The in-plane Φ scan along the <101> directions of the LBCO and LAO reveals that only the {101} reflections separated by 90° were appeared in the scan with sharp peaks, confirming that the LBCO films have excellent single crystallinity, as seen the inset of Fig 1. The in-plane relationship between the LBCO film and the LAO substrate was therefore determined to be $[100]_{LBCO}//[001]_{LAO}$ and $(001)_{LBCO}//(100)_{LAO}$. Fig. 14(a) is a cross-sectional TEM image of a LBCO film on LAO substrate. The LBCO thin film, with a thickness of ~150 nm, has a flat surface and a sharp interface. Fig. 14(b) is a selected-area EDP of an area covering the entire film and substrate taken with the electron-beam parallel to the $[010]_{LAO}$. Fig. 14(b) exhibits characteristics of a single crystal diffraction pattern of a cubic perovskite structure indicating an epitaxial growth of a cubic perovskite LBCO film. The orientation relationship between the LBCO film and LAO substrate can be identified as $(001)_{LBCO}$□$(001)_{LAO}$ and $<100>_{LBCO}$□$<100>_{LAO}$. Fig. 14(c) is a HRTEM image of a cross-sectional LBCO/LAO film

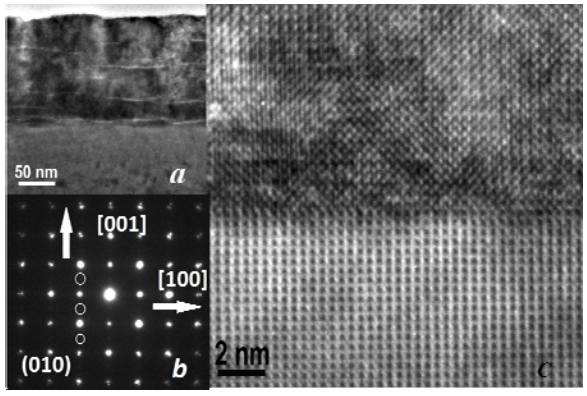

Figure 14(a) Cross-section TEM of LBCO/LAO; (b) SAED pattern from LBCO/LAO interface; (c) cross-section HRTEM of LBCO/LAO

taken with the incident electron beam parallel to the $[010]_{LAO}$ showing the microstructure near the film/substrate interface.

To understand the transport behavior of the LBCO films, resistance measurements in oxygen-hydrogen environment responses were monitored by using a high precise AC resistance bridge at 412°C. As seen in Fig. 15(a), the as-grown LBCO film was annealed in pure oxygen for three hours and the resistance reached stable status. When the gas flow was switched from oxygen into 4% hydrogen, the resistance increases drastically from $10^2\ \Omega$ to $10^7\ \Omega$, or ΔR of $10^5\ \Omega$, in the 100 ms measurement time interval. The resistance changes can be switched when alternatively change the gas environments. The detailed reduction process of the film was shown in Fig 15(b). The resistance change in the redox environment at such a short time interval suggests the LBCO is extremely sensitive to hydrogen.

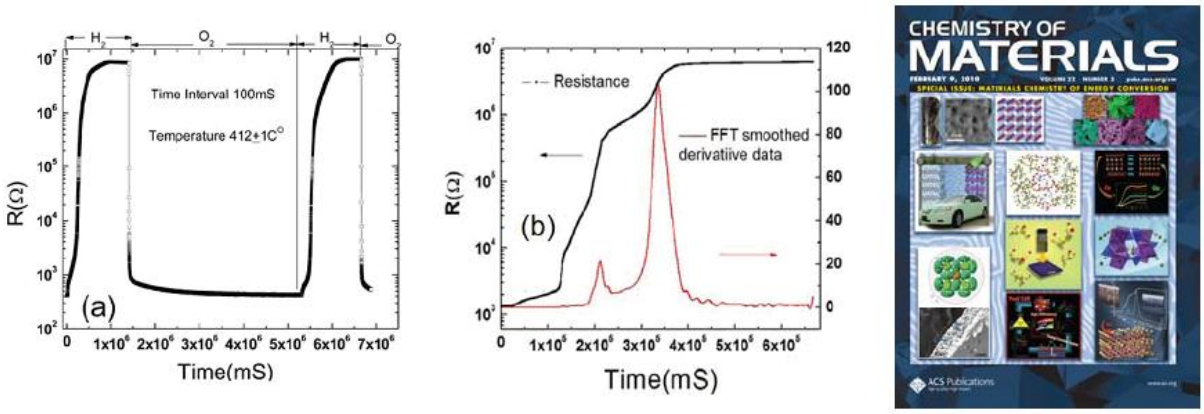

Figure 13 oxygen-hydrogen responses with reversible conducting-insolating transition monitored by resistance measurements at 412°C. (High lighted on the cover art of *Chemistry of Materials* in the lower right-hand corner.)

6. Conclusion and short comings

We have successfully demonstrated that the integration of ultra thin YSZ interlayer in the GCO thin film can significantly enhance the stability of GCO against reducing environments and reduce its the electronic conductivity. At 600 °C, electronic conductivity is only about 0.23% of the total conductivity, or 99.8% conduction are from the ionic conduction.

We achieved fabricate and characterize the epitaxial PBCO electrodes. The lowest ASR we obtained at 605°C are 0.1 $\Omega\ cm^2$ in pure oxygen and 0.18 $\Omega\ cm^2$ in air. Two cathode processes, including surface and interface, were observed. By modeling the oxygen surface exchange coeffecient, an interface region in the electrode thickness is revealed. It is also observed that the epitaxial PBCO thin film electrodes have very fast surface exchange coefficient (0.006cm/s at 598°C) and extremely low activation energy (0.28±0.04eV).

We have constructed anode supported whole cells and systematically conducted characterization and modification of electrolyte layer/ratio composition in order to maximize the ionic transport in the intermediate temperature range. The anode material used is a 50/50 cement mixture of NiO and YSZ, which has been known to have good catalytic properties. The full cell is tested in gas of a 96/4 mixture of N_2 and H_2, respectively. We have obtained a current maximum of approximately 95 mA/cm^2 with an average of 65 mA/cm^2. Calculations of the theoretical cell voltage using the Nernst equation give a voltage of approximately 1.15 volts. This research indicates that our maximum voltage of approximately 0.91V in the 96/4 mixture of

N_2 and H_2 and at 650 ^oC, suggesting that the intermediate temperature solid oxide fuel cell can be developed via integrating interface engineered multilayered structures to reduce the electronic leakage and to enhance the device performance.

Although we have demonstrated the full cell performance, the device quality is highly limited by the anode materials since the NiO/YSZ cement has large inherent porosity structures and large surface roughness which results in the current leakage and the irregularity in our cell production. We have approached to adopt various amorphous metallic ribbons with double phase structures as the anode materials, collaborated with Prof. Chuang Dong's group at the Dalian University of Technology. Due to the travel limit, we could not optimize the anode structures on time for the demonstration of the fuel cell structures. This research will be continued and will report later.

This project has supported two graduate students, Dr. Jian Liu (graduated in May 2010) and Mr. Gregory Collins, and one Hispanic undergraduate student, Mr. Emanuel Silva. This project is co-sponsored from the State of Texas through the ARP program and TcSUH and the South Texas Technology Management.

Publication List:

Patents:

1. **C. L. Chen,** G. Collins, J. Liu, "STTM No.2008.024.UTSA: Multilayered YSZ/GCO structure for intermediate temperature fuel cell applications".
2. **C. L. Chen,** and J. Liu, "STTM No. 2010.007.UTSA: Highly Epitaxail Thin Films for High Temperature/Highly Sensitive Chemical Sensors for Critical and Reducing Environment".

Refereed Journal Papers:

1) M. Liu, J. Liu, G. Collins, C. R. Ma, **C. L. Chen**,* J. He, J. C. Jiang, E.I. Meletis, A. J. Jacobson, and Q. Y. Zhang, "Magnetic and Transport properties of highly epitaxial $(LaBa)Co_2O_{5.5+\delta}$ thin films", Appl. Phys. Let., (in press)
2) J. Liu, M. Liu, G. Collins, **C. L. Chen***, X. N. Jiang, W. Q. Gong, A. J. Jacobson, J. He, J. C. Jiang, and E. I. Meletis, "Epitaxial Nature and Transport Properties in Double Perovskite $LaBaCo_2O_{5.5+\delta}$ Thin Films", **22** (2010) 799**, Chem**. **Mat.** (in press) [*with Artwork in cover page of the special issue of energy research*]
3) X. M. Xu, J. Liu, Z. Yuan, J. Weaver, **C. L. Chen,*** Y. R. Li, N. Shi, and H. J. Gao, "Single Crystalline Highly Epitaxial Pt Thin Films on (001) $SrTiO_3$", ***Appl. Phys. Lett***., **92** (2008) 102102.
4) J.C. Jiang, **C. L. Chen**, Y. Lin, J. Horwitz, A. J. Jacobson and E.I. Meletis, "Effects of Substrate Surface Local Structures on Properties and Interface Structures of Epitaxial Oxide Thin Films", Thin Solid Films, 518 (2009) 147.
5) J. Liu, X. M. Xu, G. Collins, Z. Yuan, J. Weaver, **C. L. Chen**,* G. T. Kim, A. J. Jacobson, "Strain Effects on Oxygen Transport Property in Highly Ionic Conductive $PrBaCo_2O_5$ Thin Films", ***Solid State Ionics***, (submitted).
6) J. Liu, G. Collins, M. Liu, **C. L. Chen**,* Q. Y. Zhang, and C. Dong "Highly Epitaxial LaBaCo2O5+δ Thin Films -- A Promised New Candidate for Developing High Temperature/Highly Sensitive Chemical Sensors with Critical and Reducing Environments", Adv. Mat., (submitted)
7)

Several more papers are under preparation and will be submitted for publishing soon.

GRAPHICAL MATERIALS LIST

References:

1 H. Inaba, H. Tagawa, Solid State Ionics 83 (1996) 1.

[2] S. Wang, T. Kato, S. Nagata, T. Kaneko, N. Iwashita, T. Honda and M. Dokiya, Solid State Ionics, 2002, 152–153, 477.

[3] B. C. H. Steele, Solid State Ionics, 2000, 134, 3.

[4] B. C. H. Steele, Solid State Ionics, 2000, 129, 95.

[5] T. S. Zhang, J. Ma, L. B. Kong, P. Hing and J. A. Kilner, Solid State Ionics, 2004, 167, 191.

[6] Y. J. Leng, S. H. Chan, S. P. Jiang and K. A. Khor, Solid State Ionics, 2004, 170, 9.

[7] C. Hatchwell, N. M. Sammes and I. W. M. Brown, Solid State Ionics, 1999, 126, 201.

[8] N. M. Sammes and Z. Cai, Solid State Ionics, 1997, 100, 39.

[9] S. Wang, H. Inaba, H. Tagawa, M. Dokiya and T. Hashimoto,Solid State Ionics, 1998, 107, 73.

[10] M. Mogensen, N. M. Sammes and G. A. Tompsett, Solid State Ionics, 2000, 129, 63.

[11] C. L. Chen, J. Shen, S. Y. Chen, G. P. Luo, C. W. Chu, F. A. Miranda, F.W. Van Keuls, J. C. Jiang, E. I. Meletis, and H. Chang, Appl. Phys. Lett.78, 652 ~2001

[12]Irvine, J.; Sinclair, D.; West, A.,. *Advanced Materials* **1990,** *2* (3), 132-138.

[13] *B.C.H. Steele* / *Solid State Ionics* 129 (2000) 95 –110

[14] a)Y. L. Yang,;, C. L. Chen; S. Y. Chen,; C. W. Chu,; A. J. Jacobson,, *J Electrochem Soc* **2000,** *147* (11), 4001-4007. b)Ringuede, A.; Fouletier, J.,. *Solid State Ionics* **2001,** *139* (3-4), 167-177.c) Yang, Y. M. L.; Jacobson, A. J.; Chen, C. L.; Luo, G. P.; Ross, K. D.; Chu, C. W.,. *Appl Phys Lett* **2001,** *79* (6), 776-778.

[15]T. Kawada, K. Masuda, J. Suzuki, A. Kaimai, K. Kawamura, Y. Nigara, J. Mizusaki, H. Yugami, H. Arashi, N. Sakai, H. Yokokawa, *Solid State Ionics* **1999**, 121, 271.

[16]S. Kim, S. Wang, X. Chen, Y. L. Yang, N. Wu, A. Ignatiev, A. J. Jacobson, B. Abeles, *J Electrochem Soc* **2000**, 147, 2398.

[17] G. Kim, S. Wang, A. J. Jacobson, L. Reimus, P. Brodersen, C. A. Mims, *J Mater Chem* **2007**, 17, 2500.

[18] A. Bieberle-Hutter, M. Sogaard, H. L. Tuller, *Solid State Ionics* **2006**, 177, 1969

[19]E. A. Kotomin, Y. A. Mastrikov, E. Heifetsa, J. Maier, *Physical Chemistry Chemical Physics* **2008**, 10, 4644.